NANO LETTERS

2006
Vol. 6, No. 10
2225−2231

In Vivo Molecular Probing of Cellular Compartments with Gold Nanoparticles and Nanoaggregates

Janina Kneipp,*,† Harald Kneipp,† Margaret McLaughlin,‡ Dennis Brown,‡ and Katrin Kneipp†

Wellman Center for Photomedicine, Harvard University, Medical School, Boston, Massachusetts 02114, and Renal Unit, Massachusetts General Hospital, Harvard University, Medical School, Boston, Massachusetts 02114

Received June 30, 2006; Revised Manuscript Received September 8, 2006

ABSTRACT

Surface-enhanced Raman (SERS) signatures were measured from single living cells at different times after the uptake of gold nanoparticles. The spectra are indicative of chemical changes in the environment of the nanostructures over time. The increase of the SERS signal strength and parallel TEM studies indicate the formation of nanoaggregates providing optimum SERS enhancement for ultrasensitive probing inside the endosomal compartment. The results have implications for medical and biotechnology applications of SERS nanosensors in cells.

Owing to their favorable physical and chemical properties, gold nanoparticles have been useful tools in biology for several decades. Their high electron density has made them popular labels in electron microscopy, and because their surface properties enable a great variety of functionalization procedures[1] they can be used to target selected structures in biological samples.[2−4] The latter advantage, along with the universal biocompatibility of their material, has contributed to the increasing interest in utilizing gold nanoparticles as vehicles for drug and gene delivery.[5,6] In past years, a number of studies on the behavior of gold nanoparticles in cultured cells have been conducted, investigating, for example, potential cytotoxic effects and uptake efficiency as a function of various particle parameters such as size, shape, and surface functionalization.[7−9] The plasmonic properties of gold nanoparticles allow one to detect them[10] or to measure distances between them.[11,12]

It is possible to improve spectroscopic signals from molecules in their immediate vicinity by exploiting the local optical fields of noble metal nanoparticles. Raman spectroscopy performed in the local optical fields of noble metal nanostructures, termed surface-enhanced Raman scattering (SERS),[13,14] can give detailed information on molecular structure and chemical composition in the nanometer-scaled environment of the nanoparticles.[15] In bioanalytical applications, SERS on gold nanostructures can serve two different purposes: (i) In the vast majority of experiments, they are used as SERS labels. There, a reporter molecule (e.g., a dye) linked to a gold nanoparticle is detected by its very specific Raman signature.[16] The use of SERS labels has also been demonstrated in cells, using gold or silver nanoparticles and reporter molecules.[17,18] Moreover, SERS spectra of selected reporter molecules were shown to depend on the pH value in the environment of the metal nanostructures.[19] (ii) Gold nanostructures can serve as nanosensors by delivering the enhanced Raman spectroscopic signatures of biological molecules and structures in their environment.[20,21] In general, both purposes can also be combined, and the SERS signature of a reporter on a gold nanoparticle can be obtained along with the enhanced Raman signature of its cellular environment.[17] The cellular SERS signature contains information on the molecular composition of the cellular substructure and also other chemical properties, such as the local pH. In particular, SERS nanosensors enable the chemical characterization of the nanometer vicinity of the gold nanoparticles and the measurement of vibrational spectra at a sensitivity and lateral resolution unachieved so far in other experiments.

There is compelling evidence that high SERS enhancement levels are associated mainly with enhanced local optical fields.[22,23] This implies that the SERS enhancement factor depends strongly on the morphology (e.g., the size, shape, or aggregation) of the nanoparticles. So far, the highest SERS enhancement factors have been obtained exploiting extremely high field enhancement on aggregates or clusters formed by individual silver or gold nanoparticles 20−60 nm in size.[24]

* Corresponding author. Present address: Federal Institute for Materials Research and Testing, FG I.3, Richard-Willstätter-Str. 11, D-12489 Berlin, Germany. Phone: +49-30-8104-5738. Fax: +49-30-8104-1137. E-mail: jkneipp@janina-kneipp.de.

† Wellman Center for Photomedicine, Harvard University.

‡ Renal Unit, Massachusetts General Hospital, Harvard University.

10.1021/nl061517x CCC: $33.50
Published on Web 09/23/2006

As experiments and theory show, the clusters can vary in size, ranging from dimers[25,26] to fractal structures.[27−29] Because of the important role of nanoaggregates and clusters for electromagnetic enhancement, controlling the formation of gold nanoparticle aggregates is of extreme interest for further development of SERS probing in cell biological experiments.

In this work, we investigated the behavior of gold nanoparticles in living cells and the potential of the particles to serve as SERS spectroscopic nanoprobes in a varying subcellular environment. The SERS spectra provide us with two observables: (i) the spectral signature of the SERS, which contains information on the nanometer-scaled chemical environment of the gold nanoparticles, and (ii) the signal strength of the SERS, which can give information on the SERS enhancement factor and thereby allows for the monitoring of changes in the morphology of the gold nanostructures, such as the formation of aggregates. The position of the nanoparticles with respect to cellular ultrastructure, as well as the presence and morphology of nanoaggregates in the cells, were also monitored by transmission electron microscopy (TEM).

The optimum physicochemical properties of gold nanoparticles, such as size, shape, and surface functionalization, determine which cellular barriers can be crossed by the nanoparticles, and which cellular compartment can be reached. In addition, the sub-environments found in the various cellular compartments influence the properties of the gold nanoparticles, for example, by inducing the formation of aggregates. All of these aspects need to be considered when gold nanoparticle-based SERS probes are designed for applications in living systems.

The transfer of particles into eukaryotic cells is known to work in various ways, among them fluid-phase uptake from the culture medium or mechanical methods (e.g., microinjection). As the subject of our study, we chose the endosomal system of cultured eukaryotic cells. This cellular compartment is accessible via endocytotic pathways without additional mechanical or other triggers for particle delivery. The cells take up gold nanoparticles and enclose them in endosomes. The endosomes undergo a maturation process, during which their molecular makeup changes over time, and the pH decreases and drops dramatically in the latest stage, the lysosome.[30]

Figure 1 gives a schematic description of the applied experimental procedure. The details of the experiment are described in the Supporting Information. The nanoparticles used in our study were generated by a reduction technique, as reported previously.[31] Their size ranged from 30 to 50 nm. Recently, it was shown that the endocytosis efficiency of gold nanoparticles is highest for particles of this size.[9] The electron micrograph in Figure 1B demonstrates that the gold nanoparticles were stable in cell culture medium (DMEM with 10% FCS). This medium was used for the fluid phase uptake with a nanoparticle concentration of 10^{-12} M. The observation that the particles are stable in the cell culture medium is in agreement with other recent reports, and with the well-known stabilization effects of serum proteins, the major constituents of FCS (e.g., bovine serum albumin) in experiments with cells and gold nanoparticles.[9,32,33]

The particles were delivered into cells grown on cover slips in the form of a gold pulse, lasting 30 min in immortalized rat renal proximal tubule cells (IRPT) and 60 min in the mouse macrophage cell line J774, respectively. The pulse was followed by a chase period in standard culture medium without nanoparticles (Figure 1A). In this way, with the termination of the pulse phase, no new particle uptake takes place, and the sampling of cells is based on the same amount of gold nanoparticles in the cells at all time points after the beginning of the chase period. The pulsed incubation also ensures that all endosomes containing gold nanoparticles at a specific time point exhibit a similar stage of maturation.

Figure 1C verifies that the individual particles are taken up by the cells by endocytosis. During the process of endocytosis, a part of the cellular membrane undergoes invagination, thereby enclosing a gold nanoparticle that is contained in the cell culture medium. In the cellular interior, the particle is therefore surrounded by a membrane vesicle. The transmission electron micrograph (Figure 1C) diplays a snapshot of this enclosure process as we observed it in a cell of the epithelial cell line IRPT. Endocytotic uptake of gold nanoparticles was also reported in other cell types, such as macrophages[9] and HeLa cells.[8]

After washing the cells in buffer (PBS), they were examined by Raman microspectroscopy directly in the buffer solution. During these measurements, Raman spectra were collected from individual cells in a raster scan point-by-point in a predefined grid. Excitation intensities $<3 \times 10^5$ Wcm^{-2} and the use of near-infrared excitation (786 nm) excluded possible changes in the live cells due to laser illumination. As we saw in control experiments with cells incubated in medium without gold nanoparticles, the applied low excitation intensity and 1 s collection time per spectrum do not enable the acquisition of normal Raman spectra from the cells. Only those spots where gold nanoparticles are present yield a SERS spectrum (see schematic in Figure 1D). This enabled us to selectively probe the immediate vicinity of the particles, that is, the endosomes.

We found that it was possible to measure SERS spectra from the IRPT cells as early as 10 or 20 min (i.e., during the gold pulse), a situation indicating that gold nanoparticles are associated with the epithelial cells after these time periods (spectra not shown). The electron micrographs prove an association of individual nanoparticles with microvilli of the apical membrane after ~15 min incubation with the gold.

In the following paragraphs, we discuss SERS spectra measured at different time points after the IRPT cells were subjected to a 30 min gold pulse. In general, at all time points, a scan over a cell yields different SERS spectra at different positions. However, within this variety, SERS scans performed at each different time after the pulsed incubation include specific spectral signatures with a higher probability. These spectra represent the environments of the majority of the gold nanoparticles for a specific time. Figure 2 displays for discussion the most frequent SERS spectra measured at different times after the start of the gold pulse. The typical

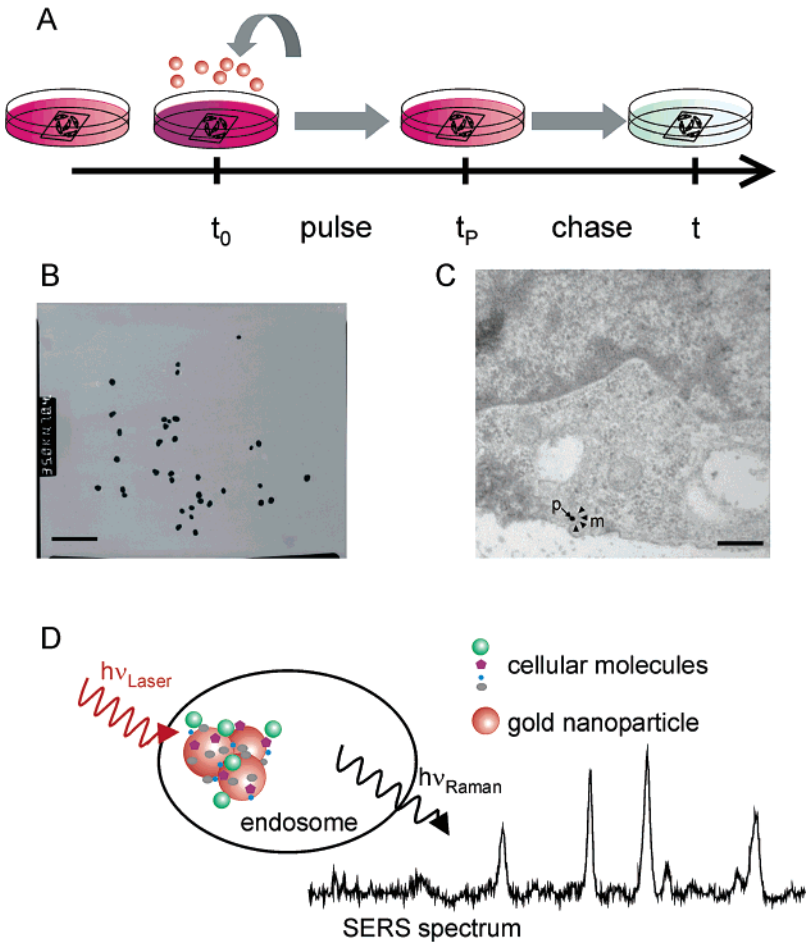

Figure 1. Schematic of the experiment. (A) Gold nanoparticles were applied with the cell culture medium at time t_0 as a pulse of duration t_P, followed by incubation in medium without nanoparticles for different times t, at which the Raman experiments were carried out in PBS buffer. (B) Transmission electron micrograph of gold nanoparticles immersed in cell culture medium (DMEM with 10% FCS). Scale bar: 500 nm. (C) Transmission electron micrograph showing the endocytotic uptake of an individual gold nanoparticle by an IRPT cell. The cell membrane (arrowheads, labeled m) encloses the particle (arrow, labeled p), thereby forming a vesicle in the cytoplasm. Scale bar: 500 nm. (D) Schematic of the SERS measurements inside the endosomal compartment. During excitation with laser light in the near-infrared ($h\nu_{Laser}$), the gold nanoparticles and nanoaggregates provide enhanced local optical fields in their nanometer-scaled vicinity, leading to surface-enhanced Raman (SERS) signals from the molecules in their immediate environment. The various vibrational modes of the different cellular molecules with energies $h\nu_{Raman}$ yield a fingerprint-like SERS spectrum.

spectral fingerprints underwent some drastic changes between the measurements performed after different time periods, suggesting changes in the chemical nanoenvironment of the particles. We will discuss these changes below.

In addition to changes in the spectral signatures, the overall strength of the SERS signals increased when the particles stayed in the cells for longer periods of time. In general, changes in the SERS signal strengths can appear because of changes in the enhancement level and/or because of changes in the number of molecules contributing to the SERS signal. In our experiments, the spectra obtained after 120 min (Figure 2C) exhibit the strongest signals. A comparison with the electron micrographs shows that the improvement in signal strengths after 120 min (Figure 2C) correlates with the formation of small gold aggregates, at that time mostly dimers and trimers (Figure 3E and F). This is in agreement with theoretical estimates showing that extremely high SERS enhancement can exist for two gold nanospheres in close proximity,[26] a situation also evidenced by our electron micrographs to exist in the endosomal structures of the epithelial cells. At later times, when the aggregates had grown further, the enhancement differed slightly from the optimum enhancement factors (compare spectra in Figure 2C with those in D and E). A rationale for this observation may be found by comparing the TEM images of the nanoclusters in the cells (Figure 3): The interparticle distances in nanoparticle accumulations after 180 min (typical example shown in Figure 3H) are greater than in the dimers and trimers (e.g., Figure 3E and F), likely because of changes in the endosomal subenvironment of the particles. Such a topological change in the endosomal ultrastructure may be due to the inclusion of the particles in multivesicular profiles that prevent the particles from coming into very close proximity (see arrow in Figure 3H). The increasing distances between the particles in the growing aggregates are different from the particle systems observed in vitro so far and would result in less optimized conditions for the electromagnetic enhancement factor that critically depends on interparticle distance.[26,34,35] The experimental results reported here strongly suggest that the observed changes in the SERS signal

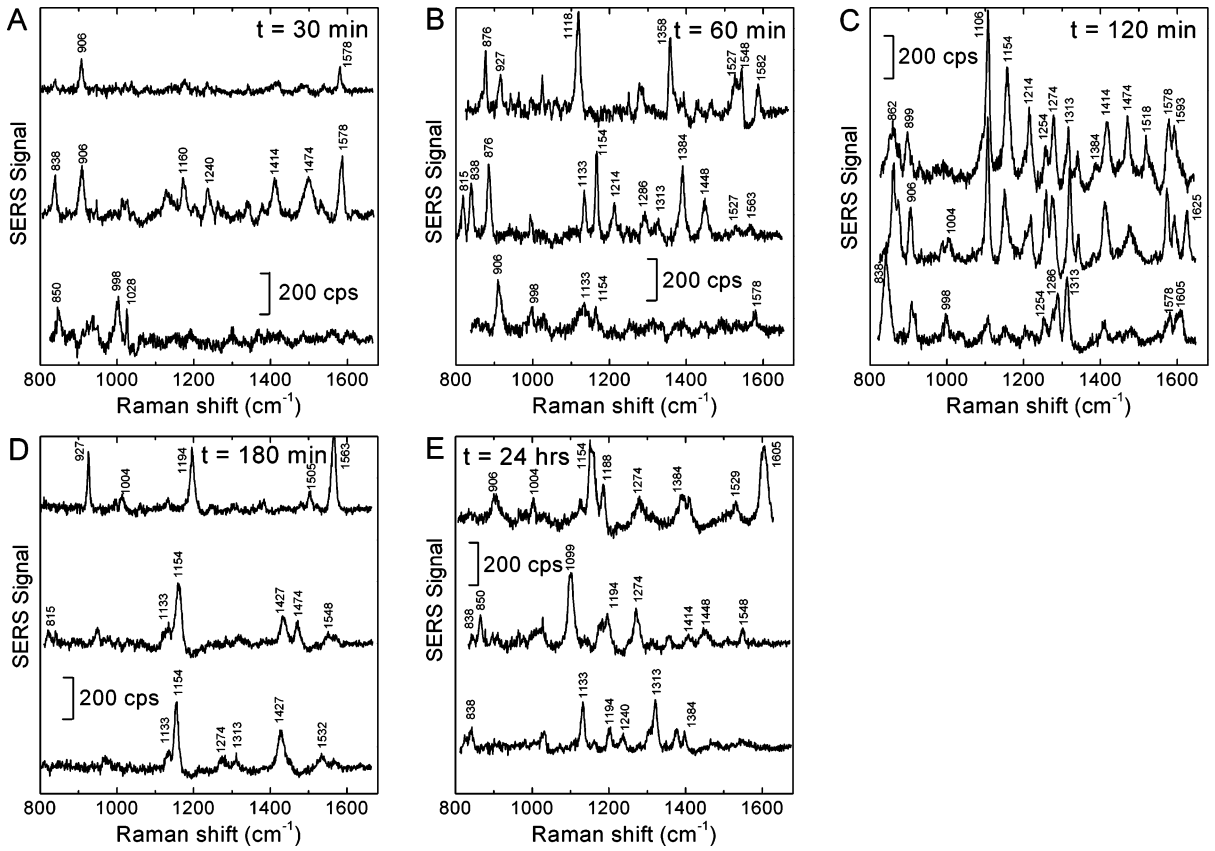

Figure 2. Typical surface-enhanced Raman (SERS) spectra from cells of the epithelial cell line IRPT after incubation with gold nanoparticles, excited with $<3 \times 10^5$ W/cm^2 at 786 nm, collection time 1 s. The incubation time, including the 30 min nanoparticle pulse, is indicated in each panel. The spectra were acquired from living cells in phosphate-buffered saline by raster scanning over individual cells using a Raman microspectroscopic setup. At the used excitation intensity and collection times, no regular Raman spectra can be observed; only spectra from positions where gold nanoparticles are present display a Raman (SERS) signal. The spectral information reflects the molecular composition in the nanometer-vicinity of the gold nanostructures, that is, of their immediate endosomal environment. The positions of the bands are labeled; please see Table 1 for an assignment of the molecular groups/ molecules that contribute to the Raman signals. Abbreviation: cps, counts per second

strengths over time are due to changes in the SERS enhancement level. As indicated by the spectra, the changes in the enhancement level are small, and the nanoaggregates present around 180 min and later (Figures 3G−J) provide an enhancement level that enables the acquisition of good signal-to-noise Raman spectra from the endosomal environment (spectra in Figure 2D and E).

As evidenced by the SERS spectral patterns contained in the data sets of ∼500−800 spectra analyzed per time point, the typical SERS fingerprints (positions and number of bands in the spectrum) changed over time, a situation that is also illustrated by the representative spectra for each time point displayed in Figure 2. The number of bands in the spectra that display 90−100% of the maximum signal level of each data set (time point) total 2−8 bands at 30 min and 4−11 bands after 60 min. The step of nanoaggregate formation leads to a significant increase in the number of spectral bands at $t = 120$ min. At this time point, the portion of SERS spectra exhibiting 90−100% of the signal level contain 13−19 characteristic bands, resulting from an abundance of different spectral contributions that were not observed for the other time points (for examples see Figure 2C). From the comparison of the 120 and 180 min spectra (see examples in Figure 2C and D), we see that there occurs again a decrease in the number of spectral features (3−6 bands in the SERS spectra of the 90−100% highest signal level). Also the spectra generated by the larger nanoaggregates (Figure 3I and J) are much less abundant with bands (Figure 2E). Table 1 lists the positions of most of the characteristic Raman frequencies of typical cellular constituents and their assignment to molecular groups and/or vibrational modes. The differences between the spectral signatures indicate that the molecular composition of the endosomal vicinity of the nanoparticles changes over time. Although the complete morphological characterization and classification of different endosomal stages is a rather complex task and not the primary objective of this study, the electron micrographs (Figure 3) suggest ultrastructural differences for the locations of the gold nanoparticles at the different time points. While after 30 min, individual gold nanoparticles could be observed associated with the plasma membrane or in small vesicles at the periphery of the cells (Figure 3A and B), the micrographs obtained at later time points suggest their presence in larger, probably multivesicular endosomes (Figure 3E−H), some of which are close to, but not in the Golgi complex (Figure 3F). At $t = 60$ min, some of the structures resemble those found for $t = 120$ min (e.g., Figure 3D), but many particles also appear in smaller profiles of

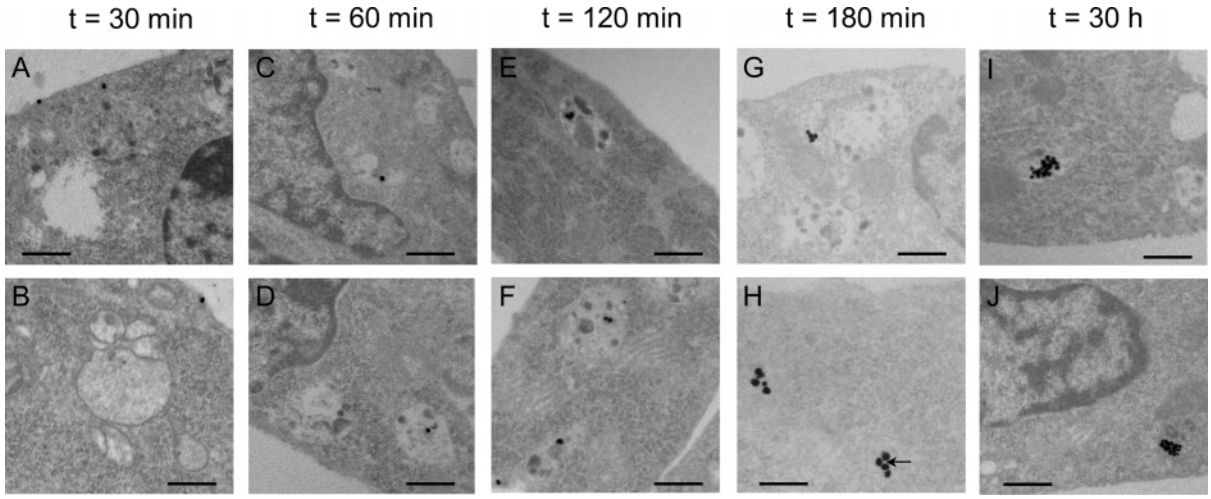

Figure 3. Transmission electron micrographs of IRPT cells at the time points of the Raman microspectroscopic experiments (compare SERS data in Figure 2). The gold nanoparticles are visible in the cells as black, electron-dense spots. The size of the nanoaggregates varies with incubation time. Nanoclusters of 2−3 particles are forming after 120 min (E, F), of 4−6 particles after 180 min (G, H), and larger lysosomal nanoaggregates during over night incubation (I, J) of the cells. The interparticle distance after 180 min is greater than that in the other time points, likely because of the enclosure of the particles in multivesicular structures (arrow indicating interparticle space). TEM images were recorded at 80 kV with a Jeol 1011 electron microscope. Scale bars: 500 nm (all except panel H). Scale bar panel H: 250 nm.

Table 1. Raman Frequencies Observed in Endosome SERS Spectra of Cell Lines IRPT and J 774 and Their Tentative Assignments to the Classes of Molecules and/or Vibrational Modes.

Raman shift (cm^{-1})	tentative assignment[a,b]
815	phosphate: ν(OPO)
827, 850	proteins, Tyr: δ(CCH) aliphatic, Tyr (ring)
862	ribose: ν(CC), ring breathing, ν(COC)
899	ribose-phosphate; saccharides
906	amino acids
927	proline: ring ν(CC)
998	proteins: amide III′
1004	Phe, ring breathing
1099	phosphate: $\nu(PO_2^-)$, ν(CC), ν(COC), glycosidic link
1106	proteins, ν(CN)
1118	proteins: ν(CN)
1133	proline
1154	ν(CC, CN), $\rho(CH_3)$
1188, 1194, 1204	nucleotides: base ν(CN), Tyr, Phe
1214, 1240, 1254	T, C, A, ring ν.
1254, 1274, 1286	proteins, lipids: amide III/ $\delta(CH_2, CH_3)$
1313	A/ proteins: ring ν/ $\gamma_T(CH_2, CH_3)$
1338, 1358	proteins: $\gamma_T(CH_2, CH_3)$, $\gamma_W(CH_2, CH_3)$
1384	nucleotides, proteins, lipids, $\delta(CH_3)$ sym
1414	amino acids, $\delta(CH_3)$ asym, $\nu(COO^-)$
1427	A, G
1448, 1474	lipids, proteins: $\delta(CH_2, CH_3)$
1505, 1518, 1532, 1578	A, C, G
1548, 1563	proteins: amide II
1582, 1593, 1605	proteins, Phe, Tyr
1625	nucleotides, lipids, proteins, ν(C=C) olefinic

[a] Based on refs 47−51. [b] Abbreviations: ν, stretching; δ, deformation; ρ, rocking; γ_T, twisting; γ_T, wagging; sym, symmetrical; asym, asymmetrical; Tyr, tyrosine; Phe, phenylalanine; A, adenine; T, thymine; C, cytosine; G, guanine.

more irregular outlines (e.g., Figure 3C). After overnight incubation, the gold nanoparticles are contained in spherical bodies, which, considering the length of the incubation time (~30 h) and the fact that all of the nanoparticles accumulate there rather than passing on to other structures, appear to be lysosomes. The differences in these endosome types suggest variation in their chemical makeup, which also reflects in the variations of the SERS spectral fingerprints that were observed for the different time points.

We performed the same SERS experiment following a 60 min gold pulse on macrophage cells (cell line J774) to test for possible dependences of the spectra on a specific cell type and to assess differences from the IRPT epithelial cell type regarding the applicability of gold nanoparticles as SERS nanosensors and regarding endosomal composition (Figure 4). Interestingly, J774 cells also show the maximum signal strengths of the SERS spectra in the time window ~120 min after incubation. This indicates that the fate of the gold nanoparticles, and in particular the formation of nanoaggregates after uptake, must be very similar in both cell lines. The results of an uptake study for gold nanoparticles of a similar size range also suggested the endocytotic mechanism for particle entry and their accumulation in lysosomes of macrophages.[8] This is also in accordance with observations and simulations of the endocytotic nanoparticle uptake by nonphagocytic cells,[36,37] and with lysosomal gold accumulations observed in J774 cells.[38] The similar behavior with respect to the SERS enhancement factor observed here provides evidence that not only uptake and final accumulation but also the endosomal trafficking of gold structures of the 30−50 nm size range must be handled in a similar fashion by epithelial cells and macrophages.

However, despite the similar behavior in nanoparticle trafficking, both cell lines are very different regarding the typical SERS signatures observed for their endosomal compartment (Figure 4). Similar to the data obtained from the IRPT cells, the spectral fingerprints contain contributions from proteins, carbohydrates, lipids, and nucleotides. Interestingly, unlike the spectra found for IRPT, a specific spectral signature appears at all time points (red spectra in Figures 4A−C), with exception of the lysosomal stage (22 h incubation). Almost all bands in this spectrum are characteristic of adenosine phosphate and show contributions from

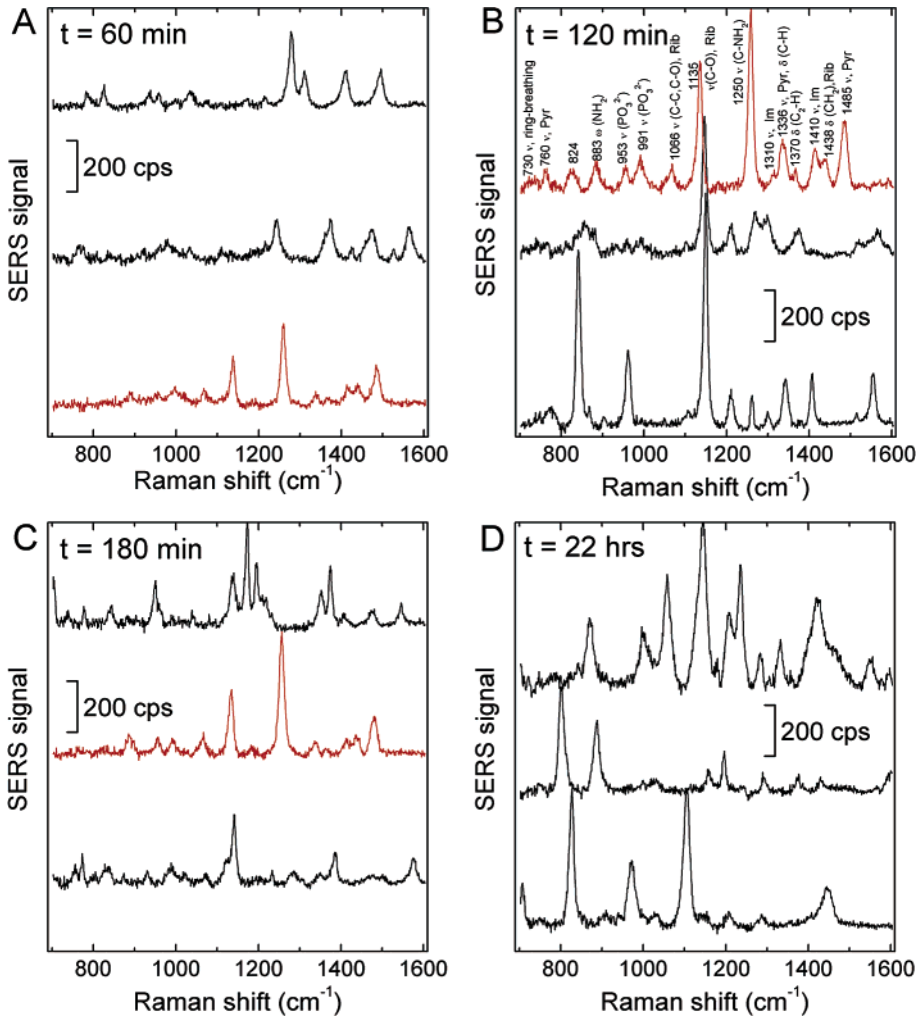

Figure 4. Typical SERS spectra collected from J774 macrophage cells after incubation with gold nanoparticles, excitation $<3 \times 10^5$ W/cm^2 at 785 nm, collection time 1 s. The incubation time, including the 60 min nanoparticle pulse, is indicated in each panel. The spectra shown in red in panels A−C represent an identical SERS fingerprint that was found at all time points and was identified as SERS spectrum of AMP and/or ATP. Band assignments based on ref 39 are indicated in panel C. Abbreviations: cps, counts per second; ν, stretching mode; ω, wagging mode;δ, bending mode; Rib, ribose; Pyr, pyrimidine; Im, imidazol

all constituents of this nucleotide (adenine, ribose, and phosphate; see band assignments in the first spectrum of Figure 4B[39]). A comparison with SERS and normal Raman data of pure AMP and ATP from the literature suggests a predominant contribution from AMP because triphosphate and diphosphate markers are absent from the spectrum.[39−41] The SERS signature of AMP was monitored in J774 cells over 180 min. During this time, the SERS signal increased by a factor of ∼2 between 60 and 120 min and then decreased within the next 60 min from this value by a factor of ∼0.6.

From the "AMP/ATP fingerprint", we can conclude that we are detecting molecular species involved in the generation of a specific endosomal milieu: The key players in the acidification and pH regulation of endosomes include an ATP-dependent proton pump and a Na-K-ATPase,[30,42] and the endosome acidification profile can be modified by cyclic AMP.[43] Nevertheless, the absence of this characteristic spectral signature from the typical spectra obtained with cell line IRPT (Figure 2) does not imply different acidification mechanisms but rather suggests differences in the regulation and composition of IRPT endosomes that are associated with the specific functions of these different cell types.

It should be noted that molecular studies of endosomes have thus far not been possible without fractionation, purification (i.e., in vitro approaches),[44,45] or the use of very few selected molecular labels in situ.[46] The experiments reported here demonstrate the potential of SERS to accomplish ultrasensitive chemical probing in individual endosomes in vivo and over time.

To summarize the major results of this work, we have measured SERS spectra from endosomes in living individual epithelial and macrophage cells and investigated the properties of gold nanoparticles in the cells. This was achieved by using the SERS spectral information itself and by complementary TEM studies. After uptake, as a consequence of their exposure to the changing endosomal environment, individual gold particles form nanoaggregates, which over time increase in size and undergo changes in morphology. Nanoparticle dimers and trimers were found to show the best SERS enhancement. Despite the influence of the cellular environment on nanoaggregate growth, nanoaggregates of all sizes

observed in the cells, as well as single nanoparticles, provide enhancement levels that allow sensitive Raman probing. Differences in the SERS spectra obtained from the molecules in the enhanced local fields of the nanostructures in different cell lines and over time, as well as the direct identification of physiologically relevant molecules, demonstrate that SERS approaches are feasible for the characterization of changing cellular environments and useful for intracellular applications.

Intracellular investigations based on SERS enable sensitive, controlled molecular probing with extremely high lateral resolution from nanometer volumes. The advantages of gold nanoparticles over other SERS substrates with respect to mobility, versatility, and biocompatibility will be useful for the development of SERS nanosensors for the probing of a variety of cellular compartments.

Acknowledgment. We thank Dennis Ausiello, Harvard Medical School, Massachusetts General Hospital Department of Medicine, for stimulating discussions. We are grateful to Ralph Peteranderl for help with cell line J774 and to Tayyabba Hasan, Wellman Center for Photomedicine, for providing us space in her cell culture facility. The help of Peggy Sherwood with the generation of the electron micrograph shown in Figure 1B is gratefully acknowledged. This work was supported by DOD grant no. AFOSR FA9550-04-1-0079 and by the generous gift of Dr. and Mrs. J. S. Chen to the optical diagnostics program of the Massachusetts General Hospital Wellman Center for Photomedicine. The Microscopy Core facility of the MGH Program in Membrane Biology (Director, Dennis Brown) receives support from an NIH Program Project Grant DK38452, the Boston Area Diabetes and Endocrinology Research Center (DK57521), and the Center for the Study of Inflammatory Bowel Disease (DK43341).

Supporting Information Available: Materials and methods. This material is available free of charge via the Internet at http://pubs.acs.org.

References

(1) Souza, G. R.; Christianson, D. R.; Staquicini, F. I.; Ozawa, M. G.; Snyder, E. Y.; Sidman, R. L.; Miller, J. H.; Arap, W.; Pasqualini, R. *Proc. Natl. Acad. Sci. U.S.A.* **2006**, *103*, 1215−1220.
(2) Feldherr, C.; Kallenbach, E.; Schultz, N. *J. Cell Biol.* **1984**, *99*, 2216−2222.
(3) Tkachenko, A. G.; Xie, H.; Liu, Y. L.; Coleman, D.; Ryan, J.; Glomm, W. R.; Shipton, M. K.; Franzen, S.; Feldheim, D. L. *Bioconjugate Chem.* **2004**, *15*, 482−490.
(4) de la Fuente, J. M.; Berry, C. C. *Bioconjugate Chem.* **2005**, *16*, 1176−1180.
(5) Sandhu, K. K.; McIntosh, C. M.; Simard, J. M.; Smith, S. W.; Rotello, V. M. *Bioconjugate Chem.* **2002**, *13*, 3−6.
(6) Han, G.; You, C. C.; Kim, B. J.; Turingan, R. S.; Forbes, N. S.; Martin, C. T.; Rotello, V. M. *Angew. Chem., Int. Ed.* **2006**, *45*, 3165−3169.
(7) Connor, E. E.; Mwamuka, J.; Gole, A.; Murphy, C. J.; Wyatt, M. D. *Small* **2005**, *1*, 325−327.
(8) Shukla, R.; Bansal, V.; Chaudhary, M.; Basu, A.; Bhonde, R. R.; Sastry, M. *Langmuir* **2005**, *21*, 10644−10654.
(9) Chithrani, B. D.; Ghazani, A. A.; Chan, W. C. W. *Nano Lett.* **2006**, *6*, 662−668.
(10) Muhlschlegel, P.; Eisler, H.-J.; Martin, O. J. F.; Hecht, B.; Pohl, D. W. *Science* **2005**, *308*, 1607−1609.
(11) Reinhard, B. M.; Siu, M.; Agarwal, H.; Alivisatos, A. P.; Liphardt, J. *Nano Lett.* **2005**, *5*, 2246−2252.
(12) Sonnichsen, C.; Reinhard, B. M.; Liphardt, J.; Alivisatos, A. P. *Nat. Biotechnol.* **2005**, *23*, 741−745.
(13) Jeanmaire, D. L.; Van Duyne, R. P. *J. Electroanal. Chem.* **1977**, *84*, 1−20.
(14) Albrecht, M. G.; Creighton, J. A. *J. Am. Chem. Soc.* **1977**, *99*, 5215−5217.
(15) Kneipp, K.; Kneipp, H.; Itzkan, I.; Dasari, R. R.; Feld, M. S. *J. Phys.: Condens. Matter* **2002**, *14*, R597−R624.
(16) Cao, Y. W. C.; Jin, R. C.; Mirkin, C. A. *Science* **2002**, *297*, 1536−1540.
(17) Kneipp, J.; Kneipp, H.; Rice, W. L.; Kneipp, K. *Anal. Chem.* **2005**, *77*, 2381−2385.
(18) Wabuyele, M. B.; Yan, F.; Griffin, G. D.; Vo-Dinh, T. *Rev. Sci. Instrum.* **2005**, *76*.
(19) Talley, C. E.; Jusinski, L.; Hollars, C. W.; Lane, S. M.; Huser, T. *Anal. Chem.* **2004**, *76*, 7064−7068.
(20) Kneipp, K.; Haka, A. S.; Kneipp, H.; Badizadegan, K.; Yoshizawa, N.; Boone, C.; Shafer-Peltier, K. E.; Motz, J. T.; Dasari, R. R.; Feld, M. S. *Appl. Spectrosc.* **2002**, *56*, 150−154.
(21) Premasiri, W. R.; Moir, D. T.; Klempner, M. S.; Krieger, N.; Jones, G.; Ziegler, L. D. *J. Phys. Chem. B* **2005**, *109*, 312−320.
(22) Moskovits, M. *J. Raman Spectrosc.* **2005**, *36*, 485−496.
(23) Kneipp, K.; Kneipp, H.; Kneipp, J. *Acc. Chem. Res.* **2006**, *39*, 443−450.
(24) Kneipp, K.; Wang, Y.; Kneipp, H.; Perelman, L. T.; Itzkan, I.; Dasari, R. R.; Feld, M. S. *Phys. Rev. Lett.* **1997**, *78*, 1667.
(25) Inoue, M.; Ohtaka, K. *J. Phys. Soc. Jpn.* **1983**, *52*, 3853−64.
(26) Xu, H. X.; Aizpurua, J.; Kall, M.; Apell, P. *Phys. Rev. E* **2000**, *62*, 4318−4324.
(27) Stockman, M. I.; Shalaev, V. M.; Moskovits, M.; Botet, R.; George, T. F. *Phys. Rev. B* **1992**, *46*, 2821.
(28) Shalaev, V. M. *Phys. Rep.* **1996**, *272*, 61−137.
(29) Yamaguchi, Y.; Weldon, M. K.; Morris, M. D. *Appl. Spectrosc.* **1999**, *53*, 127−32.
(30) Grabe, M.; Oster, G. *J. Gen. Physiol.* **2001**, *117*, 329−344.
(31) Lee, P. C.; Meisel, D. *J. Phys. Chem.* **1982**, *86*, 3391−3395.
(32) Xie, H.; Tkachenko, A. G.; Glomm, W. R.; Ryan, J. A.; Brennaman, M. K.; Papanikolas, J. M.; Franzen, S.; Feldheim, D. L. *Anal. Chem.* **2003**, *75*, 5797−5805.
(33) Bright, N. A.; Reaves, B. J.; Mullock, B. M.; Luzio, J. P. *J. Cell Sci.* **1997**, *110*, 2027−40.
(34) Li, K. R.; Stockman, M. I.; Bergman, D. J. *Phys. Rev. Lett.* **2003**, *91*, 227402.
(35) Goulet, P. J. G.; dos Santos, D. S.; Alvarez-Puebla, R. A.; Oliveira, O. N.; Aroca, R. F. *Langmuir* **2005**, *21*, 5576−5581.
(36) Rejman, J.; Oberle, V.; Zuhorn, I. S.; Hoekstra, D. *Biochem. J.* **2004**, 377, 159−169.
(37) Gao, H. J.; Shi, W. D.; Freund, L. B. *Proc. Natl. Acad. Sci. U.S.A.* **2005**, *102*, 9469−9474.
(38) da Silva, T. R. M.; de Freitas, J. R.; Silva, Q. C.; Figueira, C. P.; Roxo, E.; Leao, S. C.; de Freitas, L. A. R.; Veras, P. S. T. *Infect. Immun.* **2002**, *70*, 5628−5634.
(39) Sanchezcortes, S.; Garciaramos, J. V. *J. Mol. Struct.* **1992**, *274*, 33−45.
(40) Zhelyaskov, V.; Yue, K. T. *Biochem. J.* **1992**, *287*, 561−566.
(41) Chen, T. T.; Kuo, C. S.; Chou, Y. C.; Liang, N. T. *Langmuir* **1989**, *5*, 887−891.
(42) VanDyke, R. W. *Am. J. Physiol.* **1993**, *265*, C901−C917.
(43) Van Dyke, R. W. *Hepatology* **2000**, *32*, 1357−1369.
(44) Tjelle, T. E.; Brech, A.; Juvet, L. K.; Griffiths, G.; Berg, T. *J. Cell Sci.* **1996**, *109*, 2905−2914.
(45) Bagshaw, R. D.; Mahuran, D. J.; Callahan, J. W. *Mol. Cell. Proteomics* **2005**, *4*, 133−143.
(46) Gillooly, D. J.; Morrow, I. C.; Lindsay, M.; Gould, R.; Bryant, N. J.; Gaullier, J. M.; Parton, R. G.; Stenmark, H. *EMBO J.* **2000**, *19*, 4577−4588.
(47) Thomas, G., Jr.; Prescott, B.; Olins, D. *Science* **1977**, *197*, 385−388.
(48) Peticolas, W. L.; Patapoff, T. W.; Thomas, G. A.; Postlewait, J.; Powell, J. W. *J. Raman Spectrosc.* **1996**, *27*, 571−578.
(49) Hartman, K. A.; Clayton, N.; Thomas, G. J. *Biochem. Biophys. Res. Commun.* **1973**, *50*, 942−949.
(50) Small, E. W.; Peticolas, W. L. *Biopolymers* **1971**, *10*, 69.
(51) Parker, F. S. *Applications of Infrared, Raman, and Resonance Raman Spectroscopy in Biochemistry*; Plenum Press: New York, 1983.

NL061517X